MR. JEREMY ANDREW THOMPSON (Orcid ID : 0000-0001-9937-1888)

MR. ERIC R WENGERT (Orcid ID : 0000-0001-7679-4183)

DR. WENXI YU (Orcid ID : 0000-0003-0911-2706)

DR. IAN C. WENKER (Orcid ID : 0000-0002-0744-6510)

Title: Astrocyte Reactivity in a Mouse Model of *SCN8A* Epileptic Encephalopathy

Jeremy A. Thompson[1,2], Raquel M. Miralles[1,2], Eric R. Wengert[1,2], Pravin K. Wagley[1] Wenxi Yu[3], Ian C. Wenker[1], and Manoj K. Patel[1,2].

[1]Department of Anesthesiology, University of Virginia Health System, Charlottesville, VA

[2]Neuroscience graduate program, University of Virginia, Charlottesville, VA

[3]Department of Human Genetics, University of Michigan, Ann Arbor, MI, USA

[†]Address correspondence to mkp5u@virginia.edu.

Keywords: sodium channels, $Na_v1.6$, microglia, astrocytes, $K_{ir}4.1$, glutamine synthetase, epilepsy

ORCID numbers: Jeremy A. Thompson (0000-0001-9937-1888), Manoj K. Patel (0000-0003-3591-6716), Wenxi Yu (0000-0003-0911-2706).

Abstract

Objective: *SCN8A* epileptic encephalopathy is caused predominantly by *de novo* gain-of-function mutations in the voltage-gated-sodium channel $Na_v1.6$. The disorder is characterized by early onset of seizures and developmental delay. Most patients with *SCN8A* epileptic encephalopathy are refractory to current anti-seizure medications. Previous studies determining the mechanisms of this disease have focused on neuronal dysfunction as $Na_v1.6$ is expressed by neurons and plays a critical role in controlling neuronal excitability. However, glial dysfunction has been implicated in epilepsy and alterations in glial physiology could contribute to the pathology of *SCN8A* encephalopathy. In the current study, we examined alterations in astrocyte and microglia physiology in the development of seizures in a mouse model of *SCN8A* epileptic encephalopathy.

Methods: Using immunohistochemistry we assessed microglia and astrocyte reactivity before and after the onset of spontaneous seizures. Expression of glutamine synthetase, $Na_v1.6$ and

$K_{ir}4.1$ channel currents were assessed in astrocytes in wildtype (WT) mice and mice carrying the N1768D *SCN8A* mutation (D/+).

Results: Astrocytes in spontaneously seizing D/+ mice become reactive and increase expression of glial fibrillary acidic protein (GFAP), a marker of astrocyte reactivity. These same astrocytes exhibited reduced barium-sensitive $K_{ir}4.1$ currents compared to age-matched WT mice and decreased expression of glutamine synthetase. These alterations were only observed in spontaneously seizing mice and not before the onset of seizures. In contrast, microglial morphology remained unchanged before and after the onset of seizures.

Significance: Astrocytes, but not microglia, become reactive only after the onset of spontaneous seizures in a mouse model of *SCN8A* encephalopathy. Reactive astrocytes have reduced $K_{ir}4.1$-mediated currents, which would impair their ability to buffer potassium. Reduced expression of glutamine synthetase would modulate the availability of neurotransmitters to excitatory and inhibitory neurons. These deficits in potassium and glutamate handling by astrocytes could exacerbate seizures in *SCN8A* epileptic encephalopathy. Targeting astrocytes may provide a new therapeutic approach to seizure suppression.

Keywords: $Na_v1.6$, microglia, astrocytes, $K_{ir}4.1$, glutamine synthetase, epilepsy

Introduction

De novo missense mutations of the gene *SCN8A*, which encodes the voltage-gated sodium channel $Na_v1.6$ are associated with *SCN8A* epileptic encephalopathy [1]. Clinical features include seizure onset between 4-18 months of age, developmental delay after seizure onset, epilepsy with multiple seizure types and sudden unexpected death in epilepsy (SUDEP) in 10% of cases [2]. The expression of $Na_v1.6$ is predominantly neuronal, with high expression concentrated at the axon initial segments (AIS) and nodes of Ranvier where it promotes neuronal excitability [3–5].

Most neurologic disorders, including epilepsy, involve not just neuronal dysfunction, but also glial dysfunction. Astrocytes, in particular, play critical roles in maintaining ion and neurotransmitter homeostasis to ensure proper neuronal function [6]. During instances of insult to the brain astrocytes undergo a process termed reactive astrogliosis [7]. Reactive astrocytes display altered morphology, physiology and gene expression profile compared with astrocytes in the healthy brain, contributing to disease pathology. Several studies have demonstrated that

manipulations which produce reactive astrocytes can promote neuronal hyperexcitability [8] or lead to the development of seizures [9]. Astrocyte-specific deletion of either *KCNJ10*, encoding the inward rectifying potassium channel $K_{ir}4.1$ [10], or inhibition of the glutamate degradation enzyme glutamine synthetase (GS), facilitate the development of spontaneous seizures in mouse models [11]. Reactive astrocytes commonly downregulate these critical genes, which could contribute to brain pathology [6]. Moreover, reactive astrocytes are present in human resected tissue from patients suffering from mesial temporal lobe epilepsy (MTLE) and mutations in *KCNJ10* are causative for EAST syndrome (epilepsy, ataxia, sensorineural deafness and tubulopathy), characterized by epilepsy [12,13].

Microglia are also thought to be involved in epilepsy. In several models of temporal lobe epilepsy (TLE), microglia become reactive and contribute to seizures by the release of pro-inflammatory cytokines (IL-1β and TNF) which are pro-convulsant and microglial specific knockout of the TSC1 gene results in microglial reactivity and the development of spontaneous seizures [14]. Microglia may also have roles in regulating the ectopic neurogenesis and synaptic pruning that occurs in epilepsy [14].

In this study, we investigated whether microglia and astrocyte reactivity were associated with seizures in the N1768D mouse model of *SCN8A* encephalopathy. This model bears the first described patient point mutation, p.Asn1768Asp, and recapitulates key aspects of the disease, including the development of spontaneous seizures and an increased risk of sudden death [1,5]. We show that astrocytes become reactive in the cortex and hippocampus of spontaneously seizing mutant mice and display reduced $K_{ir}4.1$ currents, indicating an impairment in their ability to regulate extracellular K^+. Interestingly, prior to the onset of seizures, astrocytes remained quiescent and displayed unaltered $K_{ir}4.1$ currents. Astrocytes in spontaneously seizing mutant mice also exhibited reduced glutamine synthetase expression, the enzyme necessary for the conversion of glutamate to glutamine, indicating an impairment in glutamate processing. Surprisingly, microglial morphology was unchanged prior to or after the onset of spontaneous seizures. These deficits in the homeostatic functions of astrocytes, but not microglia, could contribute to the development of seizures in *SCN8A* encephalopathy, implicating a role for astrocytes in the pathology of this disease.

Materials and Methods

Animals. All experiments were performed using C57BL/6J WT mice (JAX:000664), transgenic Tg(Aldh1l1-EGFP,-DTA)D8Rth/J mice (JAX:026033) and $Scn8a^{N1768D}$ knock-in mice, referred to as D/+ [5,15]. All experiments performed on mice were conducted in compliance with the guidelines established by the National Institutes of Health's *Guide for the Care and Use of Laboratory Animals* and were approved by the University of Virginia's Institute of Animal Care and Use Committee. Both male and female mice were used in experiments. D/+ mice were genotyped as previously described [3]. To identify astrocytes Aldh1l1-EGFP and D/+ mice were crossed to create Aldh1l1-EGFP:D/+ mice. All mice were maintained on a 12-hour light/dark cycle and allowed access to food and water *ad libitum*.

Immunohistochemistry. Brain tissue for immunohistochemistry was processed as follows. Mice were anesthetized and transcardially perfused with 10 mL ice cold 1x Dulbecco's phosphate buffered saline (DPBS) followed by 10 mL ice cold 4% paraformaldehyde (PFA). Sagittal brains sections were immersed in 4% PFA for 2 hours at 4°C then stored in 1x DPBS with 0.1% sodium azide. Brains were embedded in 2% agarose and 40 μm sagittal sections were obtained using a vibratome (Leica VT1200). The following antibodies were used: rabbit polyclonal to GFAP at 1:400 (Abcam, 7260), chicken polyclonal to GFAP at 1:1000 (Abcam, 4674), goat polyclonal to IBA1 at 1:500 (Abcam, 5076), chicken polyclonal to GFP at 1:1000 (Abcam, ab13970), rabbit polyclonal to glutamine synthetase at 1:400 (Abcam, ab176562), and rabbit polyclonal to $Na_v1.6$ at 1:100 (Alomone, ASC-009). Primary antibodies were diluted in 2% goat or donkey serum depending on the secondary antibody (Jackson Immunoresearch) and 0.1% Triton-X (Sigma-Aldrich). Sections (40 μm) were stained free floating in primary antibody on a shaker at 4°C overnight. Sections were washed twice with 1x DPBS and 0.1% Triton-X. Secondary antibodies were used at 1:1000 and diluted in 2% goat or donkey serum and 0.1% Triton-X. Sections were incubated in secondary antibodies for 1 hour at room temperature on a shaker. All secondary antibodies were obtained from Invitrogen and used according to the primary antibody being detected. Tissues were counterstained with NucBlue™ Fixed Cell ReadyProbes™ Reagent (DAPI) (ThermoFisher, catalog #R37606) included in the secondary antibody solution. Tissues were mounted on slides using AquaMount (Polysciences, Inc.).

Quantification of immunohistochemistry

Imaging was performed on a Zeiss LSM 710 confocal microscope with a 20x or 63x objective. We used 3, 4 or 6 slices per mouse (field of view: FOV) to assess the percent area covered of respective immunoreactivity. During image acquisition microscope settings remained constant for WT and D/+ mice. Quantification of percent area covered was performed using ImageJ. The same threshold was applied to images from WT and D/+ mice. For Sholl analysis, brain slices were stained with the microglia/macrophage marker IBA1 and 20x images of cortical regions were acquired with the same settings for WT and D/+ mice. Fifty microglia were analyzed per mouse with 3 mice per group (WT and D/+).

Brain slice preparation for electrophysiology

Preparation of acute brain slices for electrophysiology experiments was modified from standard protocols previously described [16]. Mice were anesthetized with isoflurane and decapitated. The brains were rapidly removed and kept in chilled ACSF (0°C) containing (in mM): 125 NaCl, 2.5 KCl, 1.25 NaH_2PO_4, 2 $CaCl_2$, 1 $MgCl_2$, 0.5 L-ascorbic acid, 10 glucose, 25 $NaHCO_3$, and 2 pyruvate oxygenated with 95% O_2 and 5% CO_2. Horizontal brain slices (300 µm) of WT and D/+ mice were obtained using a vibratome (Leica VT1200) and were constantly oxygenated with 95% O_2 and 5% CO_2 throughout the preparation. Once sectioning was complete, sulforhodamine-101 (SR101) was added to the aCSF to a final dilution of 1 µM [17]. Slices were incubated in SR101 for 20 min at 34°C. Slices were then transferred to aCSF without SR101 for 10 min at 34°C to allow removal of excess SR101, before being stored at room temperature in oxygenated aCSF.

Astrocyte patch clamp recording

During recording, slices were held in a chamber perfused with heated (32°C), oxygenated aCSF. Astrocytes were identified based on uptake of SR101 using epifluorescent microscopy (Hamamatsu) and morphology using a Zeiss Axioskop 2 FS Plus microscope. Borosilicate glass pipettes (OD 1.0 mm, ID 0.58, Sarasota FL) were pulled using a Brown-Flaming puller (Model P97; Sutter Instruments). Pipettes had resistances between 4-6 MΩ when filled with an internal solution of (in mM): 130 KCl, 2 $MgCl_2$, 10 HEPES, 5 EGTA, 2 Na_2ATP, 0.5 $CaCl_2$ with pH set to 7.3 [18]. Measurements were made in whole-cell patch clamp configuration using an Axopatch

700B amplifier (Molecular Devices, pCLAMP 10.6 software) and a Digidata 1322A (Molecular Devices). To analyze potassium (K^+) currents, whole-cell patched astrocytes were voltage-clamped at -80 mV and stepped from -160 mV to 100 mV in 20 mV increments, first in aCSF without barium chloride ($BaCl_2$), then with the addition of 100 µM $BaCl_2$ to the bath. Barium-sensitive currents were determined by subtraction of currents traces in the presence of $BaCl_2$ from baseline recordings in the absence of $BaCl_2$.

Non-invasive seizure monitoring by video/EEG

To monitor spontaneous seizures, D/+ mice underwent stereotaxic (Kopf, Inc.) surgery to implant EEG headsets (Plastics1, Inc.). Surgeries were performed in accordance with the Animal Care and Use Committee guidelines at the University of Virginia, and as previously described [19]. Briefly, anesthesia was induced with 5% and maintained with 0.5%–3% isoflurane. A midline skin incision was made over the skull for electrode placement over the left and right parietal cortices. Implantation of electrodes into the brain can result in both astrocytic and microglial activation, so we used EEG leads that were attached to the outer surface of the skull, and did not penetrate the brain. These leads and the EEG headset were secured on top of the skull with dental cement. Mice were allowed to recover for a minimum of 2 days and were then housed in custom chambers with food and water *ad libitum*. EEG headsets were connected via custom cables to swivels above the chambers, allowing unrestrained movement. EEG signals were amplified at 2000x and bandpass filtered between 0.3 -100 Hz, with an analogue amplifier (Neurodata Model 12, Grass Instruments Co.). Biosignals were digitized with a Powerlab 16/35 and recorded using LabChart 7 software (AD Instruments, Inc.) at 1 kS/s. Video acquisition was performed by multiplexing four miniature night vision-enabled cameras and then digitizing the video feed with a Dazzle Video Capture Device (Corel, Inc.) and recording at 30 fps with LabChart 7 software in tandem with biosignals. Seizures were identified by cortical spike waves discharges and commensurate seizure behaviors that were all considered at least stage 5 on the modified Racine Scale [20]. A subset of mice did not receive surface EEG implantation, but were only video monitored for the presence or absence of seizure behaviors in the same way. Only mice that had on average 2-3 seizures per day for 2-4 consecutive days were used in this study.

Data analysis

Clampfit software version 10.7 was used to analysis the electrophysiological recordings. Sholl analysis was performed in ImageJ using the Sholl analysis plugin [21]. Data represent means ± standard deviation (SD). Statistical significance was determined using a Student's t-test or a standard one-way or two-way ANOVA followed by Sidak multiple comparisons (GraphPad Prism 8).

Results

Astrocytes become reactive in spontaneously seizing *SCN8A* mutant mice

Increases in the expression of the cytoskeletal protein glial fibrillary acidic protein (GFAP) is indicative of astrocyte reactivity. We therefore assessed the percent area stained for GFAP in adult WT and D/+ mice that were confirmed to be spontaneously seizing. In WT mice, few cortical astrocytes expressed GFAP (**Fig.1 A, A';** n = 5 mice). In contrast, in spontaneously

seizing adult D/+ mice, there was widespread GFAP expression in cortical astrocytes, indicative of reactivity (**Fig.1 B, B', C; Table 1;** n = 5 mice). In addition to the cortex, there was also a significant increase in GFAP expression in hippocampal astrocytes from spontaneously seizing D/+ mice (**Fig.1 E, E', F:** n = 5 mice) compared to WT (**Fig.1 D, D'; Table 1**: n = 5 mice). The increase in GFAP in cortical and hippocampal astrocytes from seizing D/+ mice could be explained by either an increase in individual astrocyte GFAP expression or by an increase in the number of cortical and hippocampal astrocytes. Since GFAP is not uniformaly expressed by all astrocytes and is only found in the astrocyte primary processes and labels astrocyte somas poorly, using GFAP to accurately assess astrocyte cell numbers is not ideal. To overcome this we used mice which express GFP under the ALDH1L1 promoter [22] (Aldh1l1-EGFP:D/+) to selectively label astrocytes in the brain and address whether the increase in GFAP expression was due to an increase in astrocyte numbers. We observed no increase in the number of GFP labelled astrocytes per FOV (6 per mouse) in either the cortex (**Fig. 1 G-I**: n = 5 mice) or hippocampus (**Fig. 1 J-L**: n = 5 mice) of spontaneously seizing D/+ mice when compared to WT age-matched controls, suggesting that there was no change in the total number of astrocytes present (**Table 1**).

Previous studies have shown that D/+ mice are susceptible to audiogenic seizures and have hyper-excitable neurons at time points before the onset of spontaneous seizures which occurs between 8-16 weeks postnatal [3,23]. To explore whether astrocyte reactivity occurred before spontaneous seizure onset we examined the percent area covered by GFAP expression in young WT (n = 5) and D/+ (n = 5) mice (P21-24; 3 FOV per mouse). In young, non-seizing D/+ mice there was no difference in cortical (**Fig. 1 M-O**) or hippocampal (data not shown) GFAP expression indicating a lack of astrocyte reactivity prior to seizure onset (**Table 1**).

Microglia reactivity is not associated with *SCN8A* epileptic encephalopathy

Microglia are the resident immune cells of the brain, as such, they are uniquely poised to respond to insults or alterations of brain homeostasis by becoming reactive. Reactive microglia are characterized by a change in morphology including reduced arbor complexity and have been detected in mouse models of seizures and in epileptic human resected tissue [24,25]. Reactive microglia exhibit a reduction in process complexity with distance from the soma which can be assessed using Sholl analysis. Staining of microglia with IBA1 showed no change in microglia

morphology in pre-seizing age D/+ mice (**Fig.2 B**) or in spontaneously seizing adult D/+ mice (**Fig.2 E**) compared to age-matched WT mice (**Fig.2 A, D**) (n= 3 WT and 3 D/+ mice, 50 cells per mouse; 3 FOV per mouse, *p*-value= 0.8156 for young mice and *p*-value= 0.7013 for seizing mice, two-way ANOVA, with Sidak multiple comparisons). No changes in process complexity with distance from soma were detected in either pre-seizing D/+ mice (**Fig.2 C**) or spontaneously seizing D/+ mice (**Fig.2 F**) compared to age-matched WT controls.

Astrocytes in spontaneously seizing *SCN8A* mice display reduced $K_{ir}4.1$ currents

Astrocyte reactivity is associated with the downregulation of genes/proteins involved in the homeostatic functions of astrocytes such as the inward rectifying $K_{ir}4.1$ channel. The $K_{ir}4.1$ channel mediates astrocytic uptake of extracellular K^+ that is released following neuronal repolarization after action potentials. Due to the importance of astrocytic $K_{ir}4.1$ channels to buffer K^+ and its potential to be downregulated in reactive astrocytes we explored $K_{ir}4.1$ currents in astrocytes from young pre-seizing, as well as adult spontaneously seizing D/+ mice. In pre-seizing mice (P23-P28) there were no significant differences in the total or $K_{ir}4.1$ currents between WT and D/+ mice (**Fig.3 A-B, E-F**) (WT; n = 11, 3 mice and D/+; n = 9, 3 mice; *p*-value = 0.2162 for total current and *p*-value = 0.0722 for $BaCl_2$-sensitive current, two-way ANOVA with Sidak multiple comparisons). In contrast, in spontaneously seizing adult D/+ mice the total current (**Fig.3 C, D**) and $K_{ir}4.1$ current (**Fig.3 G, H**) amplitudes in reactive astrocytes were significantly reduced by 30% and 36% respectively (WT; n = 10, 3 mice and D/+; n = 17, 3 mice; *p*-value = 0.0085 for total current and *p*-value = 0.0245 for $BaCl_2$-sensitive current, two-way ANOVA with Sidak multiple comparisons). These data are suggestive of a disruption in the astrocytic K^+ buffering capacity in seizing D/+ mice. Interestingly, a trend for an increase in the total and $K_{ir}4.1$ current was observed in young, pre-seizing D/+ mice.

Expression of glutamine synthetase is reduced in spontaneously seizing *SCN8A* mice

Another important function of astrocytes is the uptake of glutamate and its conversion to glutamine, a precursor for both glutamate and GABA synthesis [6]. This conversion is carried out by the enzyme glutamine synthetase (GS), which is necessary to supply neurons with neurotransmitter precursors, and to prevent the reversal of astrocyte glutamate transporters and the release of glutamate from astrocytes. Staining of GS, as defined as percent area covered, was

reduced in cortical (**Fig.4 A-C**) and hippocampal (**Fig.4 D-F**) astrocytes from spontaneously seizing D/+ (n = 6) mice compared to WT (n = 7) mice (**Table 1;** 4 FOVs per mouse). These results indicate that glutamate handling is likely impaired in spontaneously seizing D/+ mice and could contribute to pathology in this model.

Astrocytes do not express the voltage-gated sodium channel, Na$_v$1.6

Previous studies have suggested that astrocytes express Na$_v$1.6 [26–28]. Since *SCN8A* encephalopathy is caused by mutations in *SCN8A*, we investigated whether astrocytes in spontaneously seizing D/+ mice express Na$_v$1.6 using immuno-labeling techniques. As expected, Na$_v$1.6 labeled neuronal somata (asterisks) in WT (**Fig. 5 A**: n = 3 mice) and D/+ (**Fig. 5 B:** n = 3 mice) mice. However, Na$_v$1.6 did not co-localize with the astrocyte reporter GFP fluorescence in the cortex or hippocampus (data not shown). Despite *SCN8A* encephalopathy being caused by mutations in *SCN8A*, our data suggest that astrocytes do not express Na$_v$1.6 and their dysfunction in this disease is likely secondary to aberrant neuronal activity caused by neuronal expression of the mutated Na$_v$1.6.

Discussion

SCN8A encephalopathy is caused primarily by gain-of-function mutations in the neuronal sodium channel Na$_v$1.6 and causes severe, early onset seizures and SUDEP [29]. Due to the neuronal expression of Na$_v$1.6 mechanistic studies into *SCN8A* encephalopathy have focused on the impact of mutations on the excitability of excitatory and inhibitory neurons. However, there is growing appreciation for the involvement of other cell types, principally astrocytes and microglia, in epilepsy pathology [6,14]. In the current study we sought to investigate alterations in microglia and astrocytes morphology before and after the onset of spontaneous seizures in a knock-in mouse model carrying the human *SCN8A* mutation N1768D. We found that 1) astrocytes, but not microglia, become reactive in spontaneously seizing mice, 2) astrocyte reactivity is not observed at a time point before the onset of spontaneous seizures even though increases in neuronal excitability at this earlier time point have been reported [3], 3) reactive astrocytes have reduced K$_{ir}$4.1 channel currents and reduced GS expression suggesting an impairment in K$^+$ ion uptake and glutamate homeostasis and 4) astrocytes do not express Na$_v$1.6,

suggesting that changes in astrocyte physiology are in response to pro-epileptic alterations in surrounding neuronal networks. This study provides support for a previously unappreciated role for astrocytes in *SCN8A* encephalopathy.

Astrocytes are key cells that function to maintain the homeostasis of the brain through buffering ions, such as K^+, removing neurotransmitters from the extracellular space, and supporting neurons metabolically, among numerous other roles [30]. Following insults to the brain astrocytes become reactive and exhibit stereotypic changes in morphology and upregulate cytoskeletal proteins, such as GFAP and vimentin [7]. Despite these stereotypic changes, the term astrocyte "reactivity" refers to a highly heterogenous process that alters astrocyte physiology in a context dependent manner [31]. The astrocytic response to CNS insults can be either beneficial or detrimental depending on the type of astrocyte responding (i.e. protoplasmic vs. fibrous, cortical vs hippocampal), the type of eliciting event (i.e. seizure, infection, etc.) and the temporal course of the insult (i.e. early vs late stage disease) [32,33]. The Barres group demonstrated that astrocytes responding to either systemic LPS injection or middle cerebral artery occlusion (MCAO) become reactive and can be neurotoxic (A1) or neuroprotective (A2) respectively [31,34]. Subsequent work using single-cell RNAseq of isolated astrocytes from various disease models and human samples have revealed astrocyte disease-specific gene expression profiles in Huntingtin's disease (HD), Alzheimer's disease (AD) and multiple sclerosis that conform neither to the A1 nor the A2 profile [32,35–37].

While reactive astrocytes can be beneficial as in the case of spinal cord injury by forming a barrier between healthy and necrotic tissue or in *Toxoplasma gondii* infection by producing chemokines to recruit helpful immune cells, reactive astrocytes can also be detrimental [38,39]. A common feature of reactive astrocytes is the downregulation of genes involved in maintaining CNS homeostasis such as $K_{ir}4.1$, aquaporin 4 and neurotransmitter transporters and degrading enzymes [40]. Tong *et al* (2014) demonstrated that AAV-mediated restoration of reduced $K_{ir}4.1$ expression in reactive striatal astrocytes ameliorated the uncoordinated gait in an HD mouse model. Further, the inability of reactive astrocytes to regulate GABA transmission worsens murine cognition in an AD mouse model [41]. Loss of the homeostatic functions of astrocytes is the most prominent feature of reactive astrocytes in epilepsy [6,9,42].

Astrocyte reactivity is often associated with seizures and epilepsy and is considered a "hallmark feature" of MTLE [6,43]. Surgical resection of the glial scar containing reactive

astrocytes in epileptic patients alleviates the seizures [42,44,45]. There is debate regarding whether astrogliosis is a cause or consequence of seizures, but growing evidence suggests that astrocyte reactivity alone can lead to seizures [8,9] and mutations in astrocyte-specific genes can lead to epilepsy, as in the case of Alexander's disease (mutations in *GFAP*) and EAST syndrome (mutations in *KCNJ10*) [46,47]. Astrogliosis is often associated with the downregulation of genes necessary for the homeostatic functions of astrocytes such as *KCNJ10*, encoding $K_{ir}4.1$, glutamate transporters and glutamine synthetase [40,48].

The presence of reactive astrocytes in the D/+ model of *SCN8A* epileptic encephalopathy was previously reported using transcriptome analysis that detected >3-fold elevated expression of the pan-reactive astrocyte transcripts *Gfap, Vimentin,* and *Serpin3a* in forebrain of D/+ mice within 24 hours after the onset of seizures, as well as elevated GFAP staining in hippocampus [34,49]. The reactive astrocyte genes *Gfap*, *Vimentin*, and *Serpin3a* were the only astrocyte-specific transcripts detected by Sprissler *et al* (2017) from whole-forebrain homogenate and are shared by both A1 and A2 reactive astrocytes [31,34]. Neurotoxic A1 reactive astrocytes are induced by TNF and IL-1b released from activated microglia [34]. We assessed microglial reactivity in seizing D/+ mice using Sholl analysis and found no evidence for activated microglia. Therefore, the lack of microglial reactivity suggests that reactive astrocytes in seizing D/+ mice are not A1 neurotoxic astrocytes. Conversely, MCAO-induced A2 reactive astrocytes are characterized by cell cycle gene upregulation and the production of neurotrophic factors such as leukemia inhibitory factor (LIF) [31]. Our study did not directly address astrocyte proliferation, however, counts of Aldh1L1-eGFP+ cortical and hippocampal astrocytes from WT and seizing D/+ mice demonstrate no change in astrocyte numbers between these two groups. The neurotrophic factor LIF has been implicated in the pilocarpine model of seizures as a pro-inflammatory cytokine promoting microglia and astrocyte reactivity [50]. LIF knockout mice have reduced microglial and astrocyte reactivity and are more likely to survive pilocarpine-induced seizures than their WT counterparts [50]. In this context an A2 neurotrophic factor could have a seizure promoting effect. Our data indicate that reactive astrocytes in seizing D/+ mice do not conform to the A1 or A2 phenotype and future experiments utilizing RNAseq on isolated astrocytes from WT and seizing D/+ could clarify the consequences of astrocyte reactivity in SCN8A epileptic encephalopathy.

We extend these findings of Sprissler *et al* (2017) to show that in spontaneously seizing D/+ mice cortical astrocytes are also reactive and that these reactive astrocytes have reduced

$K_{ir}4.1$ channel currents, with likely deficits in K^+ buffering, and reduced glutamine synthetase expression. We also show that astrocyte reactivity or deficits in $K_{ir}4.1$ function do not precede the onset of spontaneous seizures even though pro-excitatory events have been initiated in medial entorhinal cortex neurons at this time point [3] and mice are susceptible to audiogenic seizures [23]. Metabolic stress has been shown to induce astrogliosis [51] and it is tempting to speculate that astrocytes become reactive as a consequence of increased demand to buffer excess K^+ and glutamate from hyperactive neurons after the onset of spontaneous seizures. Astrocyte reactivity may represent the tipping point in the manifestation of seizures in *SCN8A* encephalopathy, leading to the increase in seizure frequency and eventual death typical of this mouse model [52].

Astrocyte K^+ buffering through the $K_{ir}4.1$ channel is essential for proper brain function. Animal models of astrocyte-specific deletion of *KCNJ10* consistently show early mortality with seizures [10,53–55]. Ablation of $K_{ir}4.1$ impairs K^+ buffering [56] and elevated extracellular K^+ promotes neuronal excitability [18]. In humans, mutations in $K_{ir}4.1$ cause EAST syndrome [47]. Some of these mutations have been characterized as loss-of-function, thus impairing K^+ buffering through $K_{ir}4.1$ [57]. In addition to its contribution to K^+ buffering, impairment of $K_{ir}4.1$ function also reduced glutamate clearance [10,54]. This is likely due to the effect of $K_{ir}4.1$ on the very negative resting membrane potential of astrocytes and the electrogenic nature of glutamate transporters which rely on the negative membrane potential to import glutamate [10,30,53,58]. Thus, perturbations in $K_{ir}4.1$ function can contribute to seizures and epilepsy.

Our study also found that glutamine synthetase staining was reduced in spontaneously seizing D/+ mice. Glutamine synthetase is predominantly expressed by astrocytes and its function is critical for the continued uptake of glutamate by glutamate transporters and for the balance of excitatory and inhibitory tone [6,8,59]. In resected tissue from patients suffering from MTLE with hippocampal sclerosis glutamine synthetase expression is greatly reduced [60] and when an inhibitor of glutamine synthetase, methionine sulfoximine , is chronically administered to rats they develop recurrent seizures [61]. Glutamine synthetase expression is also reduced in reactive astrocytes in a slice model of seizure-like activity corresponding to a decrease in inhibitory neurotransmission, a result of a smaller pool of transmitter availability in predominantly GABAergic interneurons [8].

Lastly, we assessed whether astrocytes in spontaneously seizing D/+ mice express $Na_v1.6$ since it has been reported that astrocytes can express $Na_v1.6$ in pathological settings[27,28]. However, astrocytes in WT and spontaneously seizing D/+ mice did not express $Na_v1.6$. The lack of $Na_v1.6$ expression in astrocytes is not surprising and is likely due to the absence of Rbfox RNA-binding protein expression in astrocytes [62]. Rbfox proteins are expressed in neurons and promote the expression of full-length *Scn8a* mRNA transcripts that contain alternative exon 18A. Cells lacking Rbfox proteins, including astrocytes, express alternative exon 18N with an in-frame stop codon that results in non-sense-mediated decay of the *Scn8a* transcript and lack of expression of $Na_v1.6$ protein [62].

In conclusion, the involvement of astrocytes in the pathology of *SCN8A* epileptic encephalopathy is supported by our findings, deepening our understanding of the mechanisms of this type of epilepsy. Our findings suggest that astrocyte functions become impaired in *SCN8A* encephalopathy, contributing to the manifestation of seizures and suggest new therapeutic directions for the treatment of this debilitating disease.

Key Points Box

- Astrocytes, but not microglia, become reactive in spontaneously seizing mice expressing the human *SCN8A* mutation N1768D

- Astrocyte reactivity is not observed at a time point before the onset of spontaneous seizures even though increases in neuronal excitability have been initiated and audiogenic seizures can be induced

- Reactive astrocytes have reduced $K_{ir}4.1$ channel currents suggesting an impairment in K^+ ion uptake

- Reactive astrocytes have reduced glutamine synthetase expression suggesting impairments in glutamate homeostasis

- Astrocytes do not express $Na_v1.6$ indicating that the physiological changes observed in astrocytes are in response to increases in neuronal excitability

Acknowledgements:

Disclosure of conflict of interest: None of the authors has any conflict of interest to disclose. Experiments have been performed with all national and international guidelines. The principles outlined in the ARRIVE guidelines, Basel declaration, including the 3R concept, were considered when planning experiments. Our Animal Welfare Assurance Number is A3245-01. Ethical publication statement: We confirm that we have read the Journal's position on issues involved in ethical publication and affirm that this report is consistent with those guidelines.

References

1. Veeramah KR, O'Brien JE, Meisler MH, Cheng X, Dib-Hajj SD, Waxman SG, et al. De novo pathogenic SCN8A mutation identified by whole-genome sequencing of a family quartet affected by infantile epileptic encephalopathy and SUDEP. Am J Hum Genet. 2012; 90(3).

2. Hammer MF, Wagnon JL, Mefford HC, Meisler MH. SCN8A-Related Epilepsy with Encephalopathy. GeneReviews®. 2016.

3. Ottolini M, Barker BS, Gaykema RP, Meisler MH, Patel MK. Aberrant sodium channel currents and hyperexcitability of medial entorhinal cortex neurons in a mouse model of SCN8A encephalopathy. J Neurosci. 2017; 37(32).

4. Caldwell JH, Schaller KL, Lasher RS, Peles E, Levinson SR. Sodium channel Nav1.6 is localized at nodes of Ranvier, dendrites, and synapses. Proc Natl Acad Sci U S A. 2000; 97(10).

5. Wagnon JL, Korn MJ, Parent R, Tarpey TA, Jones JM, Hammer MF, et al. Convulsive seizures and SUDEP in a mouse model of SCN8A epileptic encephalopathy. Hum Mol Genet. 2015; 24(2).

6. Patel DC, Tewari BP, Chaunsali L, Sontheimer H. Neuron–glia interactions in the pathophysiology of epilepsy. Vol. 20, Nature Reviews Neuroscience. Nature Publishing Group; 2019. p. 282–97.

7. Escartin C, Guillemaud O, Carrillo-de Sauvage MA. Questions and (some) answers on reactive astrocytes. Vol. 67, GLIA. 2019.

8. Ortinski PI, Dong J, Mungenast A, Yue C, Takano H, Watson DJ, et al. Selective

induction of astrocytic gliosis generates deficits in neuronal inhibition. Nat Neurosci. 2010; 13(5).

9.   Robel S, Buckingham SC, Boni JL, Campbell SL, Danbolt NC, Riedemann T, et al. Reactive astrogliosis causes the development of spontaneous seizures. J Neurosci. 2015; 35(8).

10.   Djukic B, Casper KB, Philpot BD, Chin LS, McCarthy KD. Conditional knock-out of Kir4.1 leads to glial membrane depolarization, inhibition of potassium and glutamate uptake, and enhanced short-term synaptic potentiation. J Neurosci. 2007; 27(42).

11.   Zhou Y, Dhaher R, Parent M, Hu QX, Hassel B, Yee SP, et al. Selective deletion of glutamine synthetase in the mouse cerebral cortex induces glial dysfunction and vascular impairment that precede epilepsy and neurodegeneration. Neurochem Int. 2019; 123.

12.   Heuser K, Eid T, Lauritzen F, Thoren AE, Vindedal GF, Taubøll E, et al. Loss of perivascular kir4.1 potassium channels in the sclerotic hippocampus of patients with mesial temporal lobe epilepsy. J Neuropathol Exp Neurol. 2012; 71(9).

13.   Mir A, Chaudhary M, Alkhaldi H, Alhazmi R, Albaradie R, Housawi Y. Epilepsy in patients with EAST syndrome caused by mutation in the KCNJ10. Brain Dev. 2019; 41(8).

14.   Hiragi T, Ikegaya Y, Koyama R. Microglia after Seizures and in Epilepsy. Cells. 2018; 7(4).

15.   Jones JM, Meisler MH. Modeling human epilepsy by TALEN targeting of mouse sodium channel Scn8a. Genesis. 2014; 52(2).

16.   Wengert ER, Saga AU, Panchal PS, Barker BS, Patel MK. Prax330 reduces persistent and resurgent sodium channel currents and neuronal hyperexcitability of subiculum neurons in a mouse model of SCN8A epileptic encephalopathy. Neuropharmacology. 2019; 158.

17.   Schnell C, Shahmoradi A, Wichert SP, Mayerl S, Hagos Y, Heuer H, et al. The multispecific thyroid hormone transporter OATP1C1 mediates cell-specific sulforhodamine 101-labeling of hippocampal astrocytes. Brain Struct Funct. 2015; 220(1).

18.   Tong X, Ao Y, Faas GC, Nwaobi SE, Xu J, Haustein MD, et al. Astrocyte Kir4.1 ion channel deficits contribute to neuronal dysfunction in Huntington's disease model mice. Nat Neurosci. 2014; 17(5).

19.   Wagley PK, Williamson J, Skwarzynska D, Kapur J, Burnsed J. Continuous video

electroencephalogram during hypoxia-ischemia in neonatal mice. J Vis Exp. 2020; 2020(160).

20. Van Erum J, Van Dam D, De Deyn PP. PTZ-induced seizures in mice require a revised Racine scale. Epilepsy Behav. 2019; 95.

21. Derecki N, Norris G, Derecki N, Kipnis J. Microglial Sholl Analysis. Protoc Exch. 2014; .

22. Tsai HH, Li H, Fuentealba LC, Molofsky A V., Taveira-Marques R, Zhuang H, et al. Regional astrocyte allocation regulates CNS synaptogenesis and repair. Science (80-). 2012; 337(6092).

23. Wengert ER, Wenker IC, Wagner EL, Wagley PK, Gaykema RP, Shin JB, et al. Adrenergic Mechanisms of Audiogenic Seizure-Induced Death in a Mouse Model of SCN8A Encephalopathy. Front Neurosci. 2021; 15(March):1–16.

24. Wyatt-Johnson SK, Herr SA, Brewster AL. Status epilepticus triggers time-dependent alterations in microglia abundance and morphological phenotypes in the hippocampus. Front Neurol. 2017; 8(DEC).

25. Najjar S, Pearlman D, Miller DC, Devinsky O. Refractory epilepsy associated with microglial activation. Vol. 17, Neurologist. 2011.

26. Reese KA, Caldwell JH. Immunocytochemical localization of NaCh6 in cultured spinal cord astrocytes. Glia. 1999; 26(1).

27. Zhu H, Zhao Y, Wu H, Jiang N, Wang Z, Lin W, et al. Remarkable alterations of Nav1.6 in reactive astrogliosis during epileptogenesis. Sci Rep. 2016; 6.

28. Zhu H, Lin W, Zhao Y, Wang Z, Lao W, Kuang P, et al. Transient upregulation of Nav1.6 expression in the genu of corpus callosum following middle cerebral artery occlusion in the rats. Brain Res Bull. 2017; 132.

29. Meisler MH, Helman G, Hammer MF, Fureman BE, Gaillard WD, Goldin AL, et al. SCN8A encephalopathy: Research progress and prospects. Epilepsia. 2016; 57(7).

30. Verkhratsky A, Nedergaard M. Physiology of astroglia. Physiol Rev. 2018; 98(1).

31. Zamanian JL, Xu L, Foo LC, Nouri N, Zhou L, Giffard RG, et al. Genomic analysis of reactive astrogliosis. J Neurosci. 2012; 32(18).

32. Escartin C, Galea E, Lakatos A, O'Callaghan JP, Petzold GC, Serrano-Pozo A, et al. Reactive astrocyte nomenclature, definitions, and future directions. Vol. 24, Nature Neuroscience. 2021.

33.   Matias I, Morgado J, Gomes FCA. Astrocyte Heterogeneity: Impact to Brain Aging and Disease. Vol. 11, Frontiers in Aging Neuroscience. 2019.

34.   Liddelow SA, Guttenplan KA, Clarke LE, Bennett FC, Bohlen CJ, Schirmer L, et al. Neurotoxic reactive astrocytes are induced by activated microglia. Nature. 2017; 541(7638).

35.   Al-Dalahmah O, Sosunov AA, Shaik A, Ofori K, Liu Y, Vonsattel JP, et al. Single-nucleus RNA-seq identifies Huntington disease astrocyte states. Acta Neuropathol Commun. 2020; 8(1).

36.   Grubman A, Chew G, Ouyang JF, Sun G, Choo XY, McLean C, et al. A single-cell atlas of entorhinal cortex from individuals with Alzheimer's disease reveals cell-type-specific gene expression regulation. Nat Neurosci. 2019; 22(12).

37.   Wheeler MA, Clark IC, Tjon EC, Li Z, Zandee SEJ, Couturier CP, et al. MAFG-driven astrocytes promote CNS inflammation. Nature. 2020; 578(7796).

38.   Wanner IB, Anderson MA, Song B, Levine J, Fernandez A, Gray-Thompson Z, et al. Glial scar borders are formed by newly proliferated, elongated astrocytes that interact to corral inflammatory and fibrotic cells via STAT3-dependent mechanisms after spinal cord injury. J Neurosci. 2013; 33(31).

39.   Still KM, Batista SJ, O'Brien CA, Oyesola OO, Früh SP, Webb LM, et al. Astrocytes promote a protective immune response to brain Toxoplasma gondii infection via IL-33-ST2 signaling. PLoS Pathog. 2020; 16(10).

40.   Nwaobi SE, Cuddapah VA, Patterson KC, Randolph AC, Olsen ML. The role of glial-specific Kir4.1 in normal and pathological states of the CNS. Vol. 132, Acta Neuropathologica. 2016.

41.   Dossi E, Vasile F, Rouach N. Human astrocytes in the diseased brain. Vol. 136, Brain Research Bulletin. 2018.

42.   Xu S, Sun Q, Fan J, Jiang Y, Yang W, Cui Y, et al. Role of Astrocytes in Post-traumatic Epilepsy. Vol. 10, Frontiers in Neurology. 2019.

43.   Kim JH. Pathology of epilepsy. Vol. 70, Experimental and Molecular Pathology. Academic Press Inc.; 2001. p. 345–67.

44.   Robel S. Astroglial scarring and seizures: A cell biological perspective on epilepsy. Vol. 23, Neuroscientist. 2017.

45. Hubbard J, Binder DK. Astrocytes and epilepsy. 1st ed. Academic Press Inc.; 2016.

46. Messing A, Brenner M, Feany MB, Nedergaard M, Goldman JE. Alexander disease. J Neurosci. 2012; 32(15):5017–23.

47. Abdelhadi O, Iancu D, Stanescu H, Kleta R, Bockenhauer D. EAST syndrome: Clinical, pathophysiological, and genetic aspects of mutations in KCNJ10. Rare Dis. 2016; 4(1).

48. Sheldon AL, Robinson MB. The role of glutamate transporters in neurodegenerative diseases and potential opportunities for intervention. Vol. 51, Neurochemistry International. 2007.

49. Sprissler RS, Wagnon JL, Bunton-Stasyshyn RK, Meisler MH, Hammer MF. Altered gene expression profile in a mouse model of SCN8A encephalopathy. Exp Neurol. 2017; 288.

50. Holmberg KH, Patterson PH. Leukemia inhibitory factor is a key regulator of astrocytic, microglial and neuronal responses in a low-dose pilocarpine injury model. Brain Res. 2006; 1075(1).

51. Sofroniew M V. Astrogliosis perspectives. Cold Spring Harb Perspect Biol [Internet]. 2015; 7(2):1–16. Available from: http://www.ncbi.nlm.nih.gov/pubmed/25380660%0Ahttp://www.pubmedcentral.nih.gov/articlerender.fcgi?artid=PMC4315924

52. Wenker IC, Teran FA, Wengert ER, Wagley PK, Panchal PS, Blizzard EA, et al. Postictal Death Is Associated with Tonic Phase Apnea in a Mouse Model of Sudden Unexpected Death in Epilepsy. Ann Neurol. 2021; .

53. Neusch C, Papadopoulos N, Müller M, Maletzki I, Winter SM, Hirrlinger J, et al. Lack of the Kir4.1 channel subunit abolishes K+ buffering properties of astrocytes in the ventral respiratory group: Impact on extracellular K+ regulation. J Neurophysiol. 2006; 95(3).

54. Kucheryavykh Y V., Kucheryavykh LY, Nichols CG, Maldonado HM, Baksi K, Reichenbach A, et al. Downregulation of Kir4.1 inward rectifying potassium channel subunits by RNAi impairs potassium transfer and glutamate uptake by cultured cortical astrocytes. Glia. 2007; 55(3).

55. Stewart TH, Eastman CL, Groblewski PA, Fender JS, Verley DR, Cook DG, et al. Chronic dysfunction of astrocytic inwardly rectifying K+ channels specific to the neocortical epileptic focus after fluid percussion injury in the rat. J Neurophysiol. 2010; 104(6).

56. Haj-Yasein NN, Jensen V, Vindedal GF, Gundersen GA, Klungland A, Ottersen OP, et al. Evidence that compromised K + spatial buffering contributes to the epileptogenic effect of mutations in the human kir4.1 gene (KCNJ10). Glia. 2011; 59(11).

57. Reichold M, Zdebik AA, Lieberer E, Rapedius M, Schmidt K, Bandulik S, et al. KCNJ10 gene mutations causing EAST syndrome (epilepsy, ataxia, sensorineural deafness, and tubulopathy) disrupt channel function. Proc Natl Acad Sci U S A. 2010; 107(32).

58. Olsen ML, Sontheimer H. Functional implications for Kir4.1 channels in glial biology: From K + buffering to cell differentiation. Vol. 107, Journal of Neurochemistry. 2008.

59. Norenberg MD, Martinez-Hernandez A. Fine structural localization of glutamine synthetase in astrocytes of rat brain. Brain Res. 1979; 161(2).

60. Eid T, Thomas MJ, Spencer DD, Rundén-Pran E, Lai JCK, Malthankar G V., et al. Loss of glutamine synthetase in the human epileptogenic hippocampus: Possible mechanism for raised extracellular glutamate in mesial temporal lobe epilepsy. Lancet. 2004; 363(9402).

61. Eid T, Ghosh A, Wang Y, Beckström H, Zaveri HP, Lee TSW, et al. Recurrent seizures and brain pathology after inhibition of glutamine synthetase in the hippocampus in rats. Brain. 2008; 131(8).

62. O'Brien JE, Drews VL, Jones JM, Dugas JC, Barres BA, Meisler MH. Rbfox proteins regulate alternative splicing of neuronal sodium channel SCN8A. Mol Cell Neurosci [Internet]. 2012; 49(2):120–6. Available from: http://dx.doi.org/10.1016/j.mcn.2011.10.005

Tables

Table 1: Summary statistics for GFAP, GFP and GS quantification

Staining	Brain Region	WT	D/+	P value/test
GFAP	Cortex	1.48 ± 0.39% (n=5)	18.71 ± 6.03% (n=5)	P=0.0215 students *t*-test
	Hippocampus	20.05 ± 2.25% (n=5)	64.93 ± 4.08% (n=5)	P<0.0001 students *t*-test
	Cortex P21-P24	1.60 ± 0.63% (n=5)	1.60 ± 0.96% (n=5)	P=0.5476 students *t*-test
GFP	Cortex	43.93 ± 7.73 (n=5)	40.80 ± 8.57 (n=5)	P=0.7935 students *t*-test
	Hippocampus	43.87 ± 9.01 (n=5)	46.67 ± 10.71 (n=5)	P=0.8464 students *t*-test
Glutamine Synthetase	Cortex	75.75 ± 7.55% (n=7)	20.15 ± 7.33% (n=6)	P=0.0002 students *t*-test
	Hippocampus	74.45 ± 5.69% (n=7)	27.64 ± 11.24% (n=6)	P=0.0005 students *t*-test

Figure legends

Figure 1: Astrocytes become reactive after the onset of spontaneous seizures. Few cortical astrocytes express GFAP (green) in adult wildtype (WT) mice (**A, A'**). In contrast, GFAP (green) staining in spontaneously seizing D/+ mouse cortex showed an increase in reactive astrocytes (**B, B'**). A similar pattern of increased GFAP (green) staining was observed in the hippocampus of spontaneously seizing D/+ mouse (**E, E'**) compared with WT (**D, D'**). Comparison of GFAP expression as percent area covered between WT and D/+ mice in cortex (**C**) (WT: n = 5 mice and D/+: n = 5 mice, *p*-value= 0.0215, Student's *t*-test) and hippocampus (**F**) (WT: n = 5 mice and D/+: n = 5 mice, *p*-value < 0.0001, Student's *t*-test: 3 fields of view (FOV) per mouse). The overall number of astrocytes in the cortex and hippocampus were assessed in ALDH1L1-GFP mice (6 FOV per mouse). Comparison of the number of GFP$^+$

astrocytes per FOV in 20x confocal images in the cortex (**G-H**) and hippocampus (**J-K**) of ALDH1L1-GFP mice is quantified in (**I and L**) (WT: n = 5 mice and D/+: n = 5 mice, *p*-value= 0.7935 for cortex (**I**): WT: n = 5 mice and D/+: n = 5 mice, *p*-value = 0.8464 for hippocampus (**L**), Student's *t*-test). Few cortical astrocytes express GFAP in pre-seizing age (P21-P24) mice irrespective of genotype (**M-N**). Quantification of GFAP expression in pre-seizing age mice (**O**) (WT: n = 5 mice and D/+: n = 5 mice, *p*-value= 0.5476, Student's *t*-test; 3 FOV per mouse). Scale bar = 50µm, for insets 25µm.

Figure 2: Microglia remain nonreactive in seizing D/+ mice. Cortical microglia, identified by IBA1 expression, in young (**A**) and adult (**D**) wildtype (WT) mice compared with young, pre-seizing (**B**) and spontaneously seizing adult (**E**) D/+ mice. Sholl analysis of microglia (IBA1) in WT and D/+ mice (**C, F**) (n=3 mice per group: 4 FOV per mouse, 50 cells per mouse, with error bars representing SD, *p*-value= 0.8156 (**C**) and 0.7013 (**F**)). Scale bar = 50µm, for insets 25µm.

Figure 3: Astrocytes in seizing D/+ mice have reduced K$_{ir}$4.1 currents. Current/voltage (I/V) plot of total current in young (P23-28) (**A**) wildtype (WT: n = 11, 3 mice) and D/+ (n = 9, 3 mice, *p*-value = 0.2162) cortical astrocytes with representative current traces (**B**). (**C**) I/V plot of total current in adult (P80-P130) WT and spontaneously seizing D/+ mice (WT: n = 10, 3 mice and D/+: n = 17, n = 3 mice, *p*-value= 0.0085) with representative traces (**D**). (**E**) I/V plot of BaCl$_2$ sensitive K$_{ir}$4.1 current in young WT and D/+ mice WT (n = 10, 3 mice) and D/+ (n = 9, 3 mice, *p*-value = 0.0722) with representative traces (**F**). (**G**) I/V plot of BaCl$_2$ sensitive K$_{ir}$4.1 current in adult WT and spontaneously seizing D/+ mice WT (n = 10, 3 mice) and D/+ (n = 17, 3 mice, *p*-value= 0.0245) with representative current traces (**H**). Data represents mean ± SD. All statistical tests were two-way ANOVA with Sidak multiple comparisons.

Figure 4: Glutamine synthetase (GS) expression is reduced in spontaneously seizing D/+ mice. Immunohistochemistry of glutamine synthetase (GS), magenta, in astrocytes in 40 µm fixed sections of brains from wildtype (WT) cortex and hippocampus (**A**, **D**) and spontaneously seizing D/+ mouse cortex and hippocampus (**B**, **E:** 4 FOV per mouse). White arrow heads indicate faint GS labeling in D/+ astrocytes. Green staining represents ALDH1L1-GFP staining of astrocytes. Comparison of the percent of the total area in the FOV covered by GS staining in the cortex (**C**) and hippocampus (**F**) of WT and spontaneously seizing D/+ mice (n = 7 WT and n

= 6 D/+ mice per brain area, Student's *t*-test, with error bars representing SD, *p*-value= 0.0002 for cortex and *p*-value= 0.0005 for hippocampus. Data represent (mean ± SD). Scale bars = 15µm.

Figure 5: Astrocytes do not express Na$_v$1.6 in wildtype or in spontaneously seizing D/+ mice. Immunohistochemistry of ALDH1L1-GFP (green) and Na$_v$1.6 (magenta) in cortical astrocytes in 40 µm fixed sections of brains from wildtype (**A, A'**: n = 3 mice) and D/+ mice (**B, B'**: n = 3 mice). Na$_v$1.6 is expressed in neuronal soma (indicated by asterisk) in neurons, but not co-localized with ALDH1L1-GFP labelled astrocytes. Scale bars = 15µm.
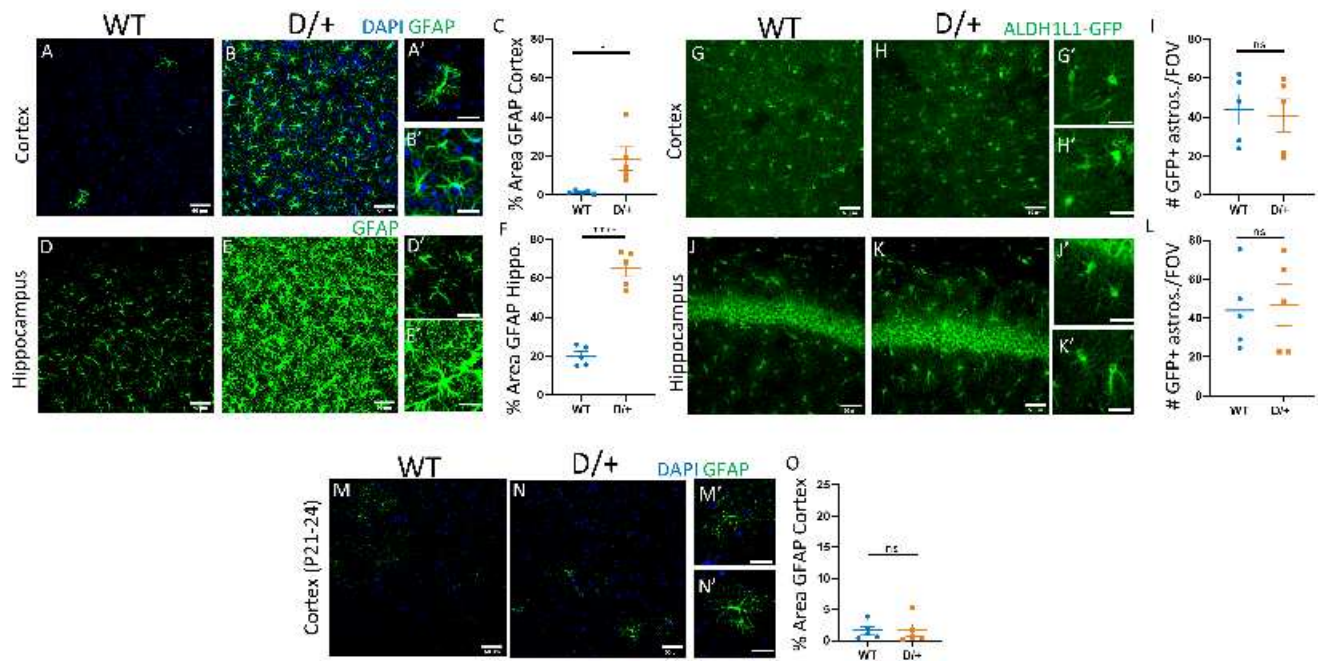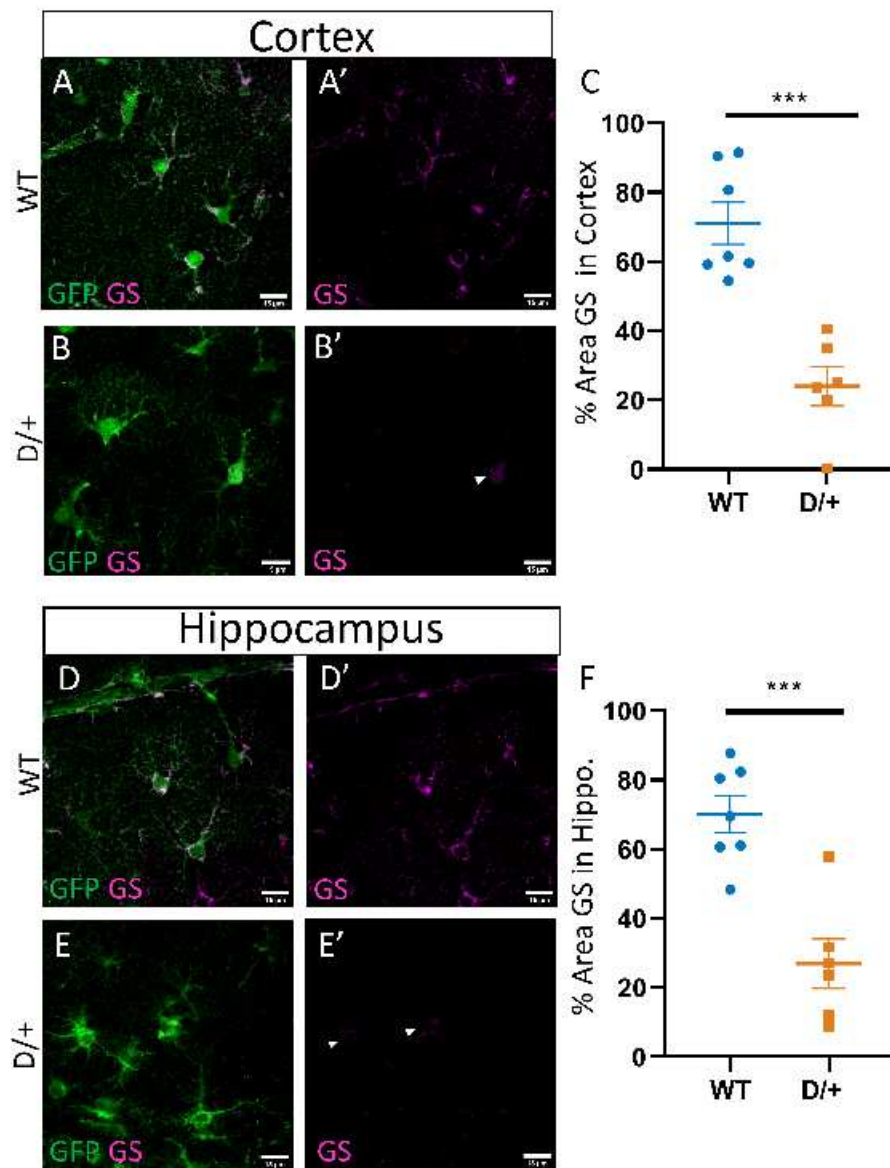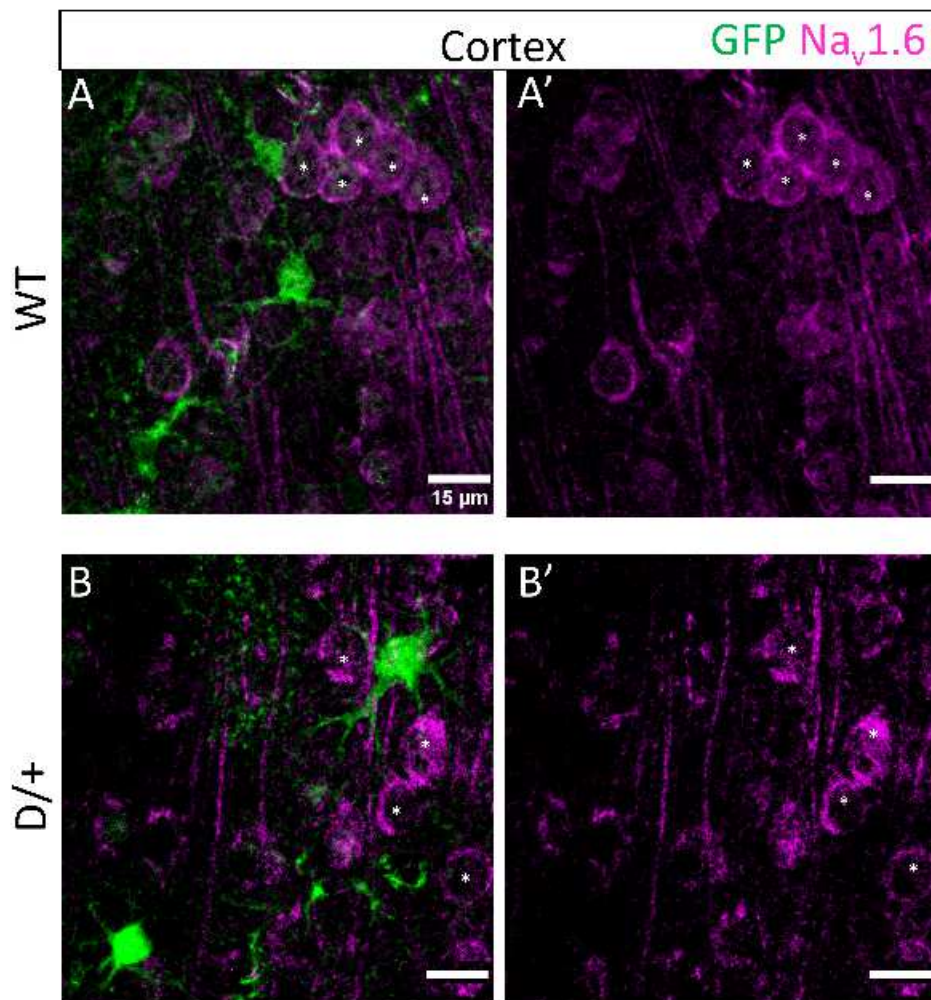
epi4_12564_f1.tif
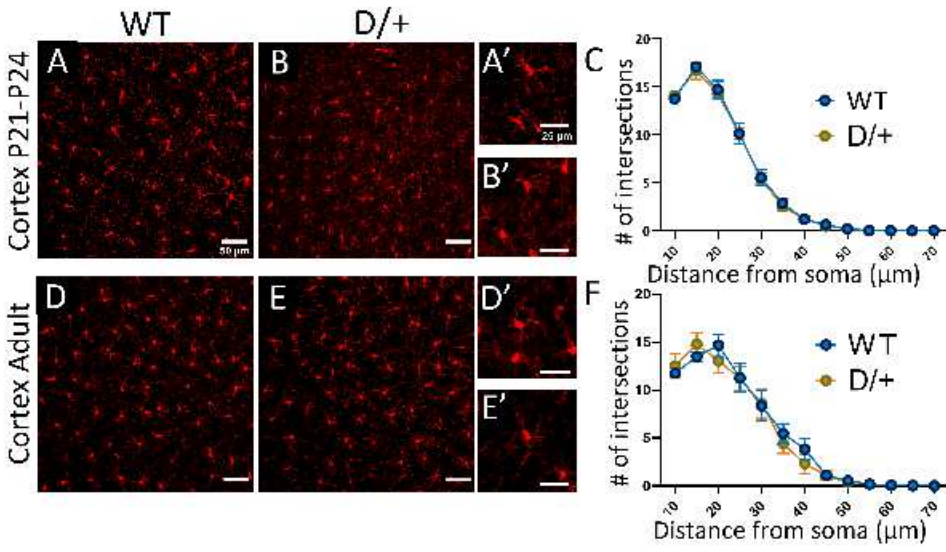
epi4_12564_f2.tif
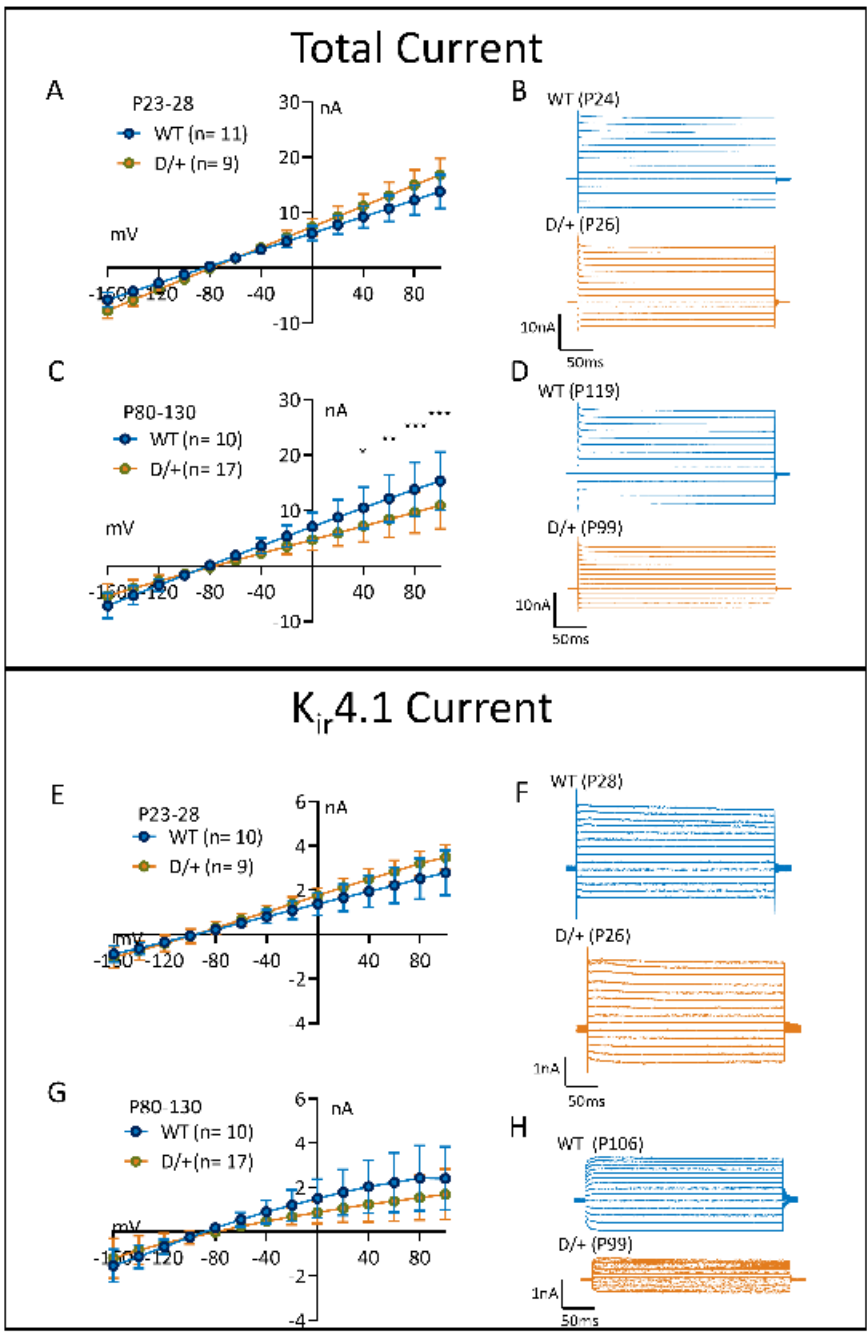
epi4_12564_f3.tif

epi4_12564_f4.tif

epi4_12564_f5.tif